Harmful Algae 18 (2012) 1–15

Contents lists available at SciVerse ScienceDirect

Harmful Algae

journal homepage: www.elsevier.com/locate/hal

Transcriptomic response of the toxic prymnesiophyte *Prymnesium parvum* (N. Carter) to phosphorus and nitrogen starvation

Sára Beszteri [a,*], Ines Yang [a,b,1], Nina Jaeckisch [a,1], Urban Tillmann [a], Stephan Frickenhaus [c,d], Gernot Glöckner [e], Allan Cembella [a], Uwe John [a]

[a] Department of Ecological Chemistry, Alfred Wegener Institute for Polar and Marine Research, Am Handelshafen 12, 27568 Bremerhaven, Germany
[b] Institute of Medical Microbiology and Hospital Epidemiology, Hannover Medical School, Carl-Neuberg-Str. 1, 30625 Hannover, Germany
[c] Computing centre/Bioinformatics, Alfred Wegener Institute for Polar and Marine Research, Am Handelshafen 12, 27568 Bremerhaven, Germany
[d] Hochschule Bremerhaven, An der Karlstadt 8, 27568 Bremerhaven, Germany
[e] Leibniz-Institute of Freshwater Ecology and Inland Fisheries, IGB, Müggelseedamm 301, D-12587 Berlin, Germany

ARTICLE INFO

Article history:
Received 23 August 2011
Received in revised form 6 March 2012
Accepted 6 March 2012
Available online 30 March 2012

Keywords:
Microarray
Golden alga
Prymnesiophyceae
Ichthyotoxic
Harmful algal bloom
Nitrogen
Phosphorus starvation

ABSTRACT

The ichthyotoxic and mixotrophic prymnesiophyte *Prymnesium parvum* is known to produce dense virtually monospecific blooms in marine coastal, brackish, and inshore waters. Fish-killing *Pyrmnesium* blooms are often associated with macronutrient imbalanced conditions based upon shifts in ambient nitrogen (N):phosphorus (P) ratios. We therefore investigated nutrient-dependent cellular acclimation mechanisms of this microalga based upon construction of a normalized expressed sequence tag (EST) library. We then profiled the transcriptome of *P. parvum* under nutrient-replete conditions as well as under nitrogen (N) and phosphorus (P) limitation via microarray analyses. Twenty-three genes putatively involved in acclimation to low nutrient levels were identified, among them three phosphate transporters, which were highly upregulated under P-starvation. In contrast, the expression of genes involved in transport and acquisition of ammonium or nitrate/nitrite was unaltered in N-starved cells. We propose that genes upregulated under P- or N-starvation lend themselves as potential tools to monitor nutrient limitation effects at the cellular level and indirectly the potential for initiation and maintenance of toxic blooms of *P. parvum*.

1. Introduction

The toxic prymnesiophyte *Prymnesium parvum* can develop massive monospecific harmful blooms worldwide, which often cause heavy economic losses through fish mortality and other types of ecosystem damage (Edvardsen and Paasche, 1998; Fistarol et al., 2003; Moestrup, 1994). These blooms are observed primarily in coastal and brackish waters, although more recently, they are frequently occurring in inland waters as well (Michaloudi et al., 2009; Baker et al., 2007; Roelke et al., 2010).

P. parvum is a rather physiologically flexible cosmopolitan species, with a wide tolerance range of salinity and temperature (Edvardsen and Imai, 2006 and references therein). Although primarily photosynthetic, this species is regarded as mixotrophic because it is able to ingest immobilized bacteria (Nygaard and Tobiesen, 1993) and other protists (Tillmann, 1998), and also takes up dissolved organic matter (Carvalho and Granéli, 2010) as a nutritional supplement.

The toxin(s) of *P. parvum* act(s) nonspecifically. The mode of action is largely undefined, but the ichthyotoxic effect is caused by increasing the permeability of gill membranes. The chemical nature of the toxin(s) also remains controversial. Igarashi et al. (1999) first isolated two polycyclic ether compounds (prymnesin 1and 2) from *P. parvum*, both of which showed potent hemolytic activity (Igarashi et al., 1999). However, a mixture of highly potent ichthyotoxic fatty acids has recently been obtained from cultured *P. parvum* cells (Henrikson et al., 2010). Moreover, these authors could not detect prymnesins in either cultured *P. parvum* cells, nor in field collected water samples during a bloom with high *P. parvum* cell concentrations accompanied by fish mortalities (Henrikson et al., 2010). They therefore concluded that uncharacterized compounds are responsible for the toxic effect of *P. parvum* rather than the polyketides prymnesin 1 or 2.

In the closely related prymnesiophyte species, *Chrysochromulina polylepis* polyunsaturated fatty acids have also been described to be responsible for lytic activity against intact cells (Yasumoto et al., 1990). However, when John et al. (2002) compared the

Abbreviations: TUG, tentative unigene; EST, expressed sequence tag; PUFA, polyunsaturated fatty acid.

* Corresponding author. Tel.: +49 471 4831 1530; fax: +49 471 4831 1425.
E-mail address: Sara.Beszteri@awi.de (S. Beszteri).

[1] These authors contributed equally.

1568-9883/$ – see front matter © 2012 Elsevier B.V. All rights reserved.
doi:10.1016/j.hal.2012.03.003

composition of fatty acid and lipid classes of toxic and non-toxic *C. polylepis* strains, no toxin-relevant difference could be detected.

Toxin production in *P. parvum* is probably intricately linked with mixotrophic nutrient acquisition strategies. The organism produces and releases toxic substances even under nutrient-replete conditions, but toxicity is increased under abiotic or biotic stress conditions including limitation of inorganic nutrients, nitrogen [N] and especially phosphorus [P] (Freitag et al., 2011; Granéli and Salomon, 2010). *Prymnesium parvum* is not able to feed on motile prey (Skovgaard and Hansen, 2003); it is supposed therefore that the role of the induced allelopathic/toxic compounds is to immobilize and lyse competing and prey algal species (Tillmann, 1998) and potential grazers (Tillmann, 2003). This strategy to kill (and then eat) its potential predators by means of toxic compounds, besides its relatively high growth rate, is thought to substantially contribute to the ability of *P. parvum* to form dense and persistent nearly monospecific toxic blooms.

In accord with this scenario, the ambient nutrient status was found to be imbalanced (high N:P ratio) during all studied *P. parvum* blooms (Kaartvedt et al., 1991; Michaloudi et al., 2009; Lindholm et al., 1999). This observation led to the assumption that the lack of available P in the water triggers enhanced cell toxicity, thereby facilitating mixotrophy and toxic bloom formation (Lindholm et al., 1999). The effect of P- and N-limitation on the exhibited toxicity of *P. parvum* has been shown in several laboratory experiments to include elevation of both intracellular (Barreiro et al., 2005; Carvalho and Granéli, 2010; Johansson and Granéli, 1999; Uronen et al., 2005) and extracellular (Graneli and Johansson, 2003; Tillmann, 2003; Uronen et al., 2007, 2005) toxicity. Details of the cellular response to low inorganic nutrient conditions are, however, still poorly understood in this species.

The biosynthetic and regulatory mechanisms associated with toxicity in *P. parvum* and nutrient-dependency of toxigenesis at the molecular level remain to be elucidated. Although no whole genome sequence is available for *P. parvum*, a normalized expressed sequence tag (EST) library has been published (La Claire, 2006). Moreover, among related prymnesiophytes, considerable comparative genomic data are now available. The complete genome of *Emiliania huxleyi* has been sequenced (http://bioinfo.c-susm.edu/Coccolithophorids/Emiliana-huxleyi), and EST libraries have been generated from *E. huxleyi* (von Dassow et al., 2009), *C. polylepis* (John et al., 2010), and *Pavlova lutheri* and *Isochrysis galbana* (Patron et al., 2006).

The recent development of high throughput transcriptomic methodologies has led to numerous investigations of the gene expressional response to nutrient limitation in various algal groups. Examples include the chlorophyte *Chlamydomonas* (Moseley et al., 2006; Wykoff et al., 1999), the prasinophyte *Micromonas* (McDonald et al., 2010), the dinoflagellate *Alexandrium minutum* (Yang et al., 2011), various diatoms (Brown et al., 2009; Parker and Armbrust, 2005), as well as the prymnesiophyte *E. huxleyi* (Bruhn et al., 2010; Dyhrman et al., 2006; Riegman et al., 2000).

In this current study, we conducted physiological experiments on growth and toxin induction and applied cDNA sequencing and microarray technology to study gene expression under N- and P-starvation in the toxic prymnesiophyte *P. parvum*. The objectives of our study were to: (1) determine physiological responses to nutrient starvation in terms of growth, toxicity and nutrient uptake; and (2) monitor the effects of nutrient starvation on *P. parvum* at the transcriptomic level and identify genes involved in the cellular response to P- and N-limitation. We investigated the transcriptomic status of *P. parvum* under nutrient deficient conditions by constructing a normalized EST library. The sequences identified served as the gene base for microarray design. The study based upon the microarray expression data provided novel insights into gene expression changes at three different growth phases of nutrient-starved and replete *P. parvum* cells in culture. This further serves as validation for the transciptomic approach to investigate potential intrinsic and extrinic factors regulating growth and bloom dynamics of HAB populations in the field.

2. Materials and methods

2.1. Culturing of algal strains

P. parvum strain RL10, isolated from Sandsfjord, Norway (Larsen and Bryant, 1998) was the subject of this study. The cryptomonad *Rhodomonas salina* (KAC 30, Kalmar Algal Collection, Kalmar, Sweden) served as a test organism in the toxicity bioassay. Cultures were grown on filter-sterilized IMR medium consisting of North Sea seawater (salinity 25 psu) enriched with macro- and micronutrients and vitamins (Eppley et al., 1967) in a controlled growth chamber at 20 °C. Illumination was provided by daylight fluorescent lamps at a photon flux density (PFD) of 200 μmol m^{-2} s^{-1} on a 16:8 light:dark photoperiod.

For cDNA library construction, *P. parvum* strain RL10 was grown in 800 ml batch cultures in 1l Erlenmeyer flasks supplied with a mixture of antibiotics (50 μg ml^{-1} penicillin, 0.025 μg ml^{-1} streptomycin sulphate, 10 μg ml^{-1} ciprofloxacin) to obtain axenic cultures. One flask was sampled daily to determine cell concentration with a Casy cell counter (Innovatis AG, Reutlingen, Germany), whereas the other three parallel cultures were harvested at the treatment-specific time point without being previously opened during the experiment. A variety of growth conditions (Table 1), including abiotic (salinity, temperature, light) and nutrient starvation-treatments were applied, in order to obtain a high diversity of expressed genes in the normalized cDNA library. Salinity was adjusted either by dilution of the seawater by deionized, filter sterilized water or by addition of NaCl to achieve the desired salinity of 5 and 50 psu, respectively. To generate P- and N-depleted cultures, KH_2PO_4 and KNO_3, respectively, were omitted from the growth medium.

Starvation experiments were carried out to study the effect of nutrient limitation on growth, toxicity and gene expression of *P. parvum*. Pre-inoculum cultures were kept in exponential growth phase by repeated sub-culturing and were treated twice for four days with an antibiotic cocktail consisting of penicillin (50 μg ml^{-1}), streptomycin sulphate (0.025 μg^{-1}) and ciprofloxacin (10 μg ml^{-1}). Before inoculating the experimental cultures, 1 ml of each inoculum stock culture was stained with Acridine orange and checked for bacterial contamination (Hobbie et al., 1977). Only cultures without evidence of bacteria were used as inoculum. Experimental cultures were grown under standard conditions as stated above in 5 l screw-cap glass bottles under gentle aeration and were sampled with a sterile tube-vacuum system (Eschbach et al., 2005).

A 15 ml subsample was taken daily for pH measurements and cell concentration was determined with a Casy cell counter

Table 1
Treatments used for the construction of the EST library.

Treatment	Salinity	Light	Temperature	Medium
	psu	μmol photons m^2 s^{-1}	(°C)	IMR
Replete control	26	200	20	IMR
Low temperature	26	200	5	IMR
High temperature	26	200	25	IMR
Low salinity	5	200	20	IMR
High salinity	50	200	20	IMR
Low light	26	7	20	IMR
P depleted	26	200	20	IMR-P
N depleted	26	200	20	IMR-N

(Innovatis AG, Reutlingen, Germany). At three time points along the growth curve, in early exponential (ca. 5×10^5 cells ml^{-1}), mid-exponential or early stationary (ca. 2×10^6 cells ml^{-1}) and in the stationary phase samples were taken for toxicity analyses, RNA extraction for microarray, and N/P measurements (particulate and dissolved). Specific growth rates (μ) were calculated as:

$$\mu = (\mathrm{In}\,(N_{t2}) - \mathrm{In}\,(N_{t1}))(t_2 - t_1)^{-1}$$

with N = cells ml^{-1} and t = sampling day.

On the last sampling day (stationary phase), two aliquots of 50 ml each of all treatments and all replicates were transferred into Erlenmeyer flasks to serve as run-on cultures for further monitoring of cell growth. To confirm nutrient limitation, one of the two aliquots per nutrient-limited culture was supplemented with the originally omitted nutrient, the other served as a follow-up control culture.

2.2. Nutrient analysis

Samples (30 ml) of filtered growth medium for dissolved nutrient analysis were preserved by adding 3 μl 3.5% (w/w) $HgCl_2$ per ml sample and stored at 4 °C until analysis. Dissolved nutrients were determined by continuous-flow analysis with photometric detection (AA3 Systems, Seal GmbH, Norderstedt, Germany). For total dissolved P and N, the analysis was preceded by digestion with peroxodisulphate in an autoclave according the standard protocol.

Samples for particulate nutrient analysis were filtered onto pre-combusted glass fibre filters (GF/F, Whatman, Omnilab, Bremen, Germany) and stored at −20 °C. Filters for C/N measurements were dried at 60 °C and encapsulated into chloroform washed tin containers. Samples were analysed on an NA 1500 C/N Analyzer (Carlo Erba Instrumentazione, Milan, Italy). Particulate phosphate was measured photometrically by continuous-flow analysis with photometric detection (AA3 Systems, Seal GmbH, Norderstedt, Germany) after digestion with peroxide and sulphuric acid (Kattner and Brockmann, 1980).

2.3. Allelopathic capacity assay

Allelochemical activity was determined by co-incubation of *P. parvum* cells with cultured cells of *R. salina* as previously described in detail (Tillmann et al., 2008). In brief, 4 ml of a mixture of *P. parvum* cells at different concentrations (2×10^3 ml^{-1}, 5×10^3 ml^{-1}, 1×10^4 ml^{-1}, 2.5×10^4 ml^{-1}, 5×10^4 ml^{-1}, 1×10^5 ml^{-1}, 2.5×10^5 ml^{-1}, 5×10^5 ml^{-1}, 1×10^6 ml^{-1} and undiluted) and *R. salina* (final cell concentration 1×10^4 ml^{-1}) were incubated in glass scintillation vials at 20 °C for 24 h in darkness. Vials were then gently mixed by rotating, and 1 ml of the mixture was pipetted into an Utermöhl cell sedimentation chamber and fixed with gluteraldehyde (1% final concentration). After settling, cells were viewed via epifluorescence microscopy (Zeiss Axiovet 2 Plus, Carl Zeiss AG, Göttingen, Germany) with Zeiss filter-set 14 at 400× magnification and intact *R. salina* cells were counted. Control *R. salina* samples in triplicate represented 0% lysis, and the effective concentration that causes 50% lysis (EC_{50}) for all samples incubated with *P. parvum* was calculated based on this control value, as percentage of *R. salina* cells lysed. The EC_{50} was estimated in a Bayesian statistical framework by fitting the following model to the cell count data using the general purpose Markov Chain Monte Carlo (MCMC) sampler OpenBUGS (Lunn et al., 2009):

$$N_{\mathrm{final}} \sim \mathrm{binomial}(p, N_{\mathrm{total}})$$

$$N_{\mathrm{total}} \sim \mathrm{poisson}(N_{\mathrm{real}})$$

$$N_{\mathrm{control}} \sim \mathrm{poisson}(N_{\mathrm{real}})$$

$$p = \frac{1}{1 + (x/\log \mathrm{EC}_{50})^h}$$

where N_{final} = *R. salina* cell concentration after incubation with *P. parvum* cells, N_{control} = *R. salina* cell concentration after incubation without *P. parvum* cells, x = log-transformed cell concentration of *P. parvum*; N_{total} = the (unknown) total number of *Rhodomonas* cells in the experiment; N_{real} = the (unknown) expectation for the latter. In a hierarchical fashion, the log EC_{50} and h values for the three replicate cultures were assumed to have been drawn from a common distribution (normal in the case of h, and log-normal for log EC_{50}). We used uninformative normal hyperpriors on the means of these distributions, and a flat gamma (0.001, 0.001) for their precision (=the inverse of the variance). The prior on N_{real} was a flat (precision = 0.001) normal distribution centred on N_{control}. The model was fitted separately to each sampling/treatment combination (i.e., three replicates each) using three chains with overdispersed random starting values. The initial 30,000 MCMC iterations were discarded as burn-in, and 1000 further samples were recorded every 20th iteration for posterior inference. Convergence was checked visually as well as using the Gelman–Rubin statistic and by comparing posterior inferences from multiple runs. Results are expressed as the posterior median of EC_{50} and their 95% highest posterior density intervals.

2.4. Intracellular toxicity measurement

Measurements of intracellular toxicity, defined as due to components normally retained within *Prymnesium* cells, were carried out as detailed in (Eschbach et al., 2001). In brief, an aliquot containing 1×10^7 cells from each culture was centrifuged at $4000 \times g$ for 10 min at 20 °C. The cell pellet was resuspended in 1 ml of the assay buffer (150 mM NaCl, 3.2 mM KCl, 1.25 mM $MgSO_4$, 3.75 mM $CaCl_2$ and 12.2 mM TRIS base, pH adjusted to 7.4 with HCl). Cells were then ultrasonicated for 1 min (50% pulse, cycle; 70% amplitude) with a sonicator (Bandelin Sonopuls, Bandelin Electronic, Berlin, Germany). 100 μl of the lysed cell suspension was incubated with an equal volume of fish erythrocytes (5×10^6 cells). After 24 h incubation, hemolytic activity was determined by measuring absorbance at 540 nm in an Ultrospec III UV/visible photometer with Wavescan Application Software (Pharmacia LKB Biotechnology, Uppsala, Sweden). A standard hemolytic curve was prepared from a saponin dilution series in the assay buffer. Results are expressed as nanogram saponin equivalents per cell (ng SnE cell^{-1}) utilizing the standard saponin from higher plants (Sigma–Aldrich, Hamburg, Germany) as an indicator of relative lytic capacity. The heterogeneity of the intercellular toxicity results across treatments and sampling time points was tested in a two-way ANOVA, and in subsequent pairwise t tests with Benjamini–Hochberg correction of significance levels accounting for multiple testing.

2.5. RNA extraction

P. parvum cultures (50 ml) were harvested in a swinging-bucket rotor centrifuge (Eppendorf 5810, Hamburg, Germany) by centrifugation for 8 min at $3000 \times g$ at 20 °C. The supernatant was discarded, the cell pellet resuspended in 500 μl lysis buffer (buffer RLT, RNeasy Plant mini Kit, Qiagen, Hilden, Germany) and immediately frozen in liquid N_2. Pellets were stored at −80 °C until

RNA extraction. Directly before RNA extraction, the resuspended cells were lysed twice for 30 s each with a TissueLyser II (Qiagen, Hilden, Germany). Total RNA extraction was performed with the RNeasy Plant mini Kit (Qiagen, Hilden, Germany), according to the manufacturer's instructions, by performing the optional DNase digestion on the spin column. RNA purity was assessed by UV-spectrophotometry at 260/230 and 260/280 nm wavelength in a Nano-drop ND-1000 spectrophotometer (Peqlab, Erlangen, Germany). RNA integrity was assessed using a 2100 Bioanalyzer (Agilent Technologies, Boeblingen, Germany).

2.6. cDNA library construction, EST sequencing and microarray analysis

2.6.1. cDNA library construction and EST sequencing and annotation

Total RNA (4550 ng) of each treatment as listed in Table 1 was pooled and sent to Vertis Biotechnologie AG (Freising-Weihenstephan, Germany) for cDNA library construction. The cDNA was synthesized according to their standard protocol for full-length enriched cDNA synthesis from poly A+ RNA purified from the total RNA and finally electroporated into competent *Escherichia coli* cells, resulting in an estimated total of 1.4×10^6 clones in the primary library.

Approximately 11×10^3 colonies were picked, and DNA was extracted by magnetic beads on a robotic platform (Qiagen, Hildesheim, Germany). Plasmid inserts were sequenced from both ends using Big Dye Chemistry (Applied Biosystems, Darmstadt, Germany) and separated on an ABI Prism 3700xl sequencer (Applied Biosystems, Darmstadt, Germany). In total 18,428 sequencing reactions were performed of which 15,591 passed the quality check and were considered as ESTs for the annotation pipeline. These were clustered with a sequential assembly using decreasing identity thresholds (gap4 assembler, Staden Package) to avoid mis-assemblies due to polyA tails. Clustering of all ESTs yielded 6381 contigs and singletons of good quality.

Contig and singleton sequences were loaded into the SAMS (Sequence Analysis and Management System, Center for Biotechnology, University of Bielefeld) for automated annotation based on BLAST comparisons against KEGG, KOG, SwissProt, InterPro and the Genbank nt and nr databases. Metabolic enzyme coding transcripts were identified using the metaSHARK tool (Pinney et al., 2005) with settings adapted to detect gene fragments (genewise run with the –init wing option).

2.6.2. Comparative analysis with other prymnesiophytes

For comparison, we performed the same analysis with the transcript sequences available for *I. galbana* (Patron et al., 2006) *E. huxleyi* (http://genome.jgi-psf.org) and for the previously published EST library from *P. parvum* (La Claire, 2006). Contig sequence data from cDNA libraries and transcript model data from the genome sequencing project for *E. huxleyi* at JGI were analysed in functional categories, applying trpsblastn (Altschul et al., 1997) against KOG/euNOG databases of eukaryote-specific sequence orthologies from eggNOG (Muller et al., 2010). Significant best hits (*e*-value $<10^{-10}$) were tabulated contig-wise and counts of common functions were computed and displayed as Venn-diagrams in R (Team, 2008) using the gplots R-package from CRAN (http://cran.r–project.org/web/packages/gplots/index.html).

KOG and euNOG databases of reference alignments from the Eggnog-2 website (version 2, http://eggnog.embl.de//) were downloaded and converted into rpsblast-formatted databases. For this purpose HMMer (Eddy, 1998) was applied to emit consensus sequences from the HMM-models of the alignments obtained from hmmbuild. Alignments were converted to position-specific scoring matrices (PSSMs) by blastpgp, using the consensus sequence as query. The resulting collections of PSSMs were assembled into rpsblast-compatible databases for the KOG and euNOG subsets of orthologies via formatrpsdb. HMMer version 2.3.2 was used in combination with BLAST programs of version 2.2.16.

To test how typical the representation of individual groups of orthologous proteins in our EST data was as compared to other haptophytes with available genomic/EST data sets, we fit a lognormal model to the proportion of tentative unique protein coding genes represented by each COG/eggnog category. We then simulated 1000 values from the fitted distributions, multiplied these expected proportions by the total number of unigenes obtained from our library, and compared these to the observed counts from our EST data for the corresponding orthogroup category. We inferred a significant departure from previous haptophyte gene inventories when the observed count for *P. parvum* lay in the 5% tails, i.e., outside the interval between the 2.5 and 97.5 percentiles of the simulated distribution.

2.6.3. Oligonucleotide design

Based on the assembled EST dataset, 60-nucleotide-hybridization probes were designed for all annotated and non-annotated contigs, at intervals of about 250 bp along the DNA sequence, oriented both in 5′-3′ and in 3′-5′ direction. The resulting 21,570 oligonucleotide sequences were synthesized on a 44k microarray. Based on the hybridization signal 2–3 probes per contig were selected. The selection criteria were reproducibility of the signal within the triplicate of arrays, as monitored by self hybridization. Final microarrays for gene expression profiling were generated by applying the selected subset of probes by Agilent (Agilent Technologies, Palo Alto, CA) using the SurePrint technology in the 44k format.

2.6.4. Microarray experiment

A "reference sample" approach was used for the microarray hybridization experiments to enable relative gene expression level comparisons across all treatments (Alizadeh et al., 2000). The reference sample consisted of a mix of *P. parvum* RNA samples, originating from different treatments also applied for the cDNA library synthesis, to obtain a reference gene expression level on as many genes as possible (Xu et al., 2002). All arrays were hybridized and analysed in biological triplicates, i.e., originating from three independent batch cultures.

The two-colour microarray-based gene expression analysis protocol and equipment employed according to recommendations of the manufacturer (Agilent Technologies, Waldbronn, Germany). 250 ng of total RNA was amplified, reverse-transcribed and labelled with the two-colour low RNA Input Fluorescent Linear Amplification kit (Agilent Technologies, Waldbronn, Germany). The Cy-3 and Cy-5 dye incorporation was verified by NanoDrop ND-1000 spectrophotometer. Hybridization was performed onto 4×44k microarray slides, with the two colour gene expression hybridization kit in SureHyb Hybridization Chambers in a hybridization oven at 65 °C for 17 h. Microarrays were scanned by an Agilent Scanner (Waldbronn, Germany). Raw data were extracted with the Agilent Feature Extraction Software version 9.5. Feature extraction software served to remove spots that had been flagged 'outliers', 'not known' or 'bad', based on background median analysis (Storey, 2003).

The program MeV (Saeed et al., 2006) was used for statistical analyses of the microarray data. To ensure statistical and biological significance, gene expression differences that proved statistically significant according to a SAM (Statistical Analysis of Microarray) analysis and showing at least two-fold expression differences between treatment and control were identified.

3. Results

3.1. EST library and functional annotation

3.1.1. Prymnesium parvum non-redundant genes

Pooling of total RNA samples isolated from different treatments (Table 1) yielded a high diversity of transcripts and allowed construction of a normalized cDNA library for *P. parvum*.

After sequencing, quality clipping and assembly 6381 tentative unique genes (TUG) were identified.

Further profile-based functional annotation of the generated TUGs for metabolic enzymes, using the metashark tool with an *e*-value cut-off of 10^{-5}, identified 392 TUGs as members of KEGG metabolic pathways (annotated with EC numbers). Analysis of the EST library published by La Claire (2006), using the same protocol and stringency, yielded annotation for 372 genes. 187 EC numbers were present in both libraries, whilst 185 EC numbers were unique to the previously published data set, and 205 were unique to the library described here. Altogether, the number of KEGG metabolic enzymes identified from *P. parvum* has been expanded from 372, based upon the EST library constructed by La Claire (2006), to 597 in the present analysis (Table 2). KEGG metabolic pathways represented by ESTs from either *Prymnesium* library are depicted in Table 2.

Twelve and six pathways (represented by 21 and 29 enzymes) were found in our and in the previous EST library, respectively, which were not present in the other *P. parvum* library (Table 3).

3.1.2. Comparative analysis of prymnesiophytes

BLAST-based sequence comparisons performed with five sets of prymnesiophyte EST libraries, specifically *I. galbana* (Patron et al., 2006), *P. lutheri* (Patron et al., 2006), *C. polylepis* (John et al., 2010), *P. parvum* I (La Claire, 2006), and *P. parvum* II (this study) and the transcript sequences of *E. huxleyi* (http://bioinfo.csusm.edu/

Table 2
Comparison of KEGG pathway genes found in the two *P. parvum* libraries.

	KEGG pathway	EC numbers ESTTAL	EC numbers Library La Claire
map00950	Alkaloid biosynthesis I	2	1
map00960	Alkaloid biosynthesis II	1	1
map00520	Amino sugar and nucleotide sugar metabolism	3	3
map00970	Aminoacyl-tRNA biosynthesis	5	7
map00330	Arginine and proline metabolism	12	14
map00053	Ascorbate and aldarate metabolism	4	5
map00410	beta-Alanine metabolism	3	4
map00100	Biosynthesis of steroids	12	6
map01040	Biosynthesis of unsaturated fatty acids	3	6
map00532	Chondroitin sulphate biosynthesis	1	1
map00020	Citrate cycle (TCA cycle)	9	11
map00460	Cyanoamino acid metabolism	4	2
map00272	Cysteine metabolism	3	1
map00982	Drug metabolism – cytochrome P450	3	3
map00983	Drug metabolism – other enzymes	4	4
map00061	Fatty acid biosynthesis	4	4
map00062	Fatty acid elongation in mitochondria	2	4
map00071	Fatty acid metabolism	6	9
map00051	Fructose and mannose metabolism	10	9
map00052	Galactose metabolism	6	6
map00361	gamma-Hexachlorocyclohexane degradation	3	2
map00480	Glutathione metabolism	9	7
map00010	Glycolysis/Gluconeogenesis	12	15
map00534	Heparan sulphate biosynthesis	4	2
map00340	Histidine metabolism	3	1
map00903	Limonene and pinene degradation	1	1
map00540	Lipopolysaccharide biosynthesis	2	1
map00300	Lysine biosynthesis	3	4
map00310	Lysine degradation	7	8
map01100	Metabolic pathways	95	221
map00980	Metabolism of xenobiotics by cytochrome P450	2	3
map00271	Methionine metabolism	3	4
map00760	Nicotinate and nicotinamide metabolism	1	1
map00401	Novobiocin biosynthesis	1	1
map00770	Pantothenate and CoA biosynthesis	1	4
map00040	Pentose and glucuronate interconversions	5	4
map00030	Pentose phosphate pathway	8	10
map00360	Phenylalanine metabolism	5	2
map00400	Phenylalanine, tyrosine and tryptophan biosynthesis	4	6
map00523	Polyketide sugar unit biosynthesis	1	1
map00860	Porphyrin and chlorophyll metabolism	6	8
map00230	Purine metabolism	47	26
map00240	Pyrimidine metabolism	38	2
map00830	Retinol metabolism	1	1
map00450	Selenoamino acid metabolism	5	4
map00500	Starch and sucrose metabolism	3	1
map00521	Streptomycin biosynthesis	1	3
map00072	Synthesis and degradation of ketone bodies	2	3
map00430	Taurine and hypotaurine metabolism	1	3
map00380	Tryptophan metabolism	6	5
map00350	Tyrosine metabolism	7	6
map00290	Valine, leucine and isoleucine biosynthesis	17	18

Table 3
Enzymes identified in the two *P. parvum* libraries which are not present in the other library.

ESTTAL	EC numbers
Benzoate degradation via hydroxylation	2
Biosynthesis of vancomycin group antibiotics	1
Caffeine metabolism	8
Carotenoid biosynthesis	1
D-Alanine metabolism	1
D-Arginine and D-ornithine metabolism	1
Glycosaminoglycan degradation	1
Indole and ipecac alkaloid biosynthesis	1
Keratan sulphate biosynthesis	1
Penicillin and cephalosporin biosynthesis	1
Puromycin biosynthesis	1
Terpenoid biosynthesis	2
Library La Claire, 2006	
Biosynthesis of ansamycins	1
Caprolactam degradation	2
Diterpenoid biosynthesis	1
Folate biosynthesis	1
Geraniol degradation	1
Phosphatidylinositol signaling system	23

Table 4
Statistics of EST sequences from cDNA libraries of species used for the analysis.

Species	Contigs	Significant hits	Median contig length
Prymnesium parvum	6381	2953	818
Prymnesium parvum	3380	1563	790
Isochrysis galbana	12,276	3686	489
Chrysochromulina polylepis	2207	707	745
Pavlova lutheri	13,068	5264	490
Emiliania huxleyi	39,126	18,699	903

Coccolithophorids/Emiliana-huxleyi/http://genome.jgi-psf.org), revealed many congruencies and apparent homologies (Table 4). In comparison to existing prymnesiophyte sequences, 2882 found hits with an *e*-value better than 10^{-5} in the *E. huxleyi* genome, compared with 1820 and 1179 in the EST libraries of *P. parvum* (La Claire, 2006) and *I. galbana* (Patron et al., 2006), respectively.

When comparing the five EST libraries, 1526 genes were found in common among these four prymnesiophytes. Furthermore, the two *P. parvum* libraries had 88 functions in common, which appear to have no counterpart in the other species investigated in this study (Fig. 1). Comparison between the transcript sequences of *E. huxleyi* and the four other prymnesiophyte species showed that 478 functions are present in all species. A further 1695 functions were only found in *P. parvum* and *E. huxleyi*, and an additional seven orthologies were shared between the EST libraries of the two toxic species *P. parvum* and *C. polylepis* (Fig. 2).

The contigs found in the EST libraries and the transcript sequences from *E. huxleyi* were annotated and sorted into KOG functional categories (Fig. 3).

Interestingly, in the category J (translation, ribosomal structure and biogenesis), we obtained less contigs than are present in the other libraries, whereas our combined *P. parvum* set of ESTs represents more functions involved in defence mechanisms (category V) than either *P. lutheri* or *I. galbana* (Fig. 3). However, altogether, the proportions of unique genes annotated as belonging to different orthologous group categories as defined in the COG/eggnogg database were in the range expected based on an identical annotation of other available haptophyte EST/genomic data sets at $p = 0.95$.

3.1.3. Genes involved in nitrogen or phosphorus metabolism, vesicle transport and growth

We searched the tentative unigene (TUG) set for genes that are hypothesized to be related to the metabolism, uptake and storage of the nutrients N and P (Table 5), cell division and growth (Table 6), as well as vesicle transport/phagotrophy (Table 7). In the case of genes putatively involved in nutrient metabolism, eighteen

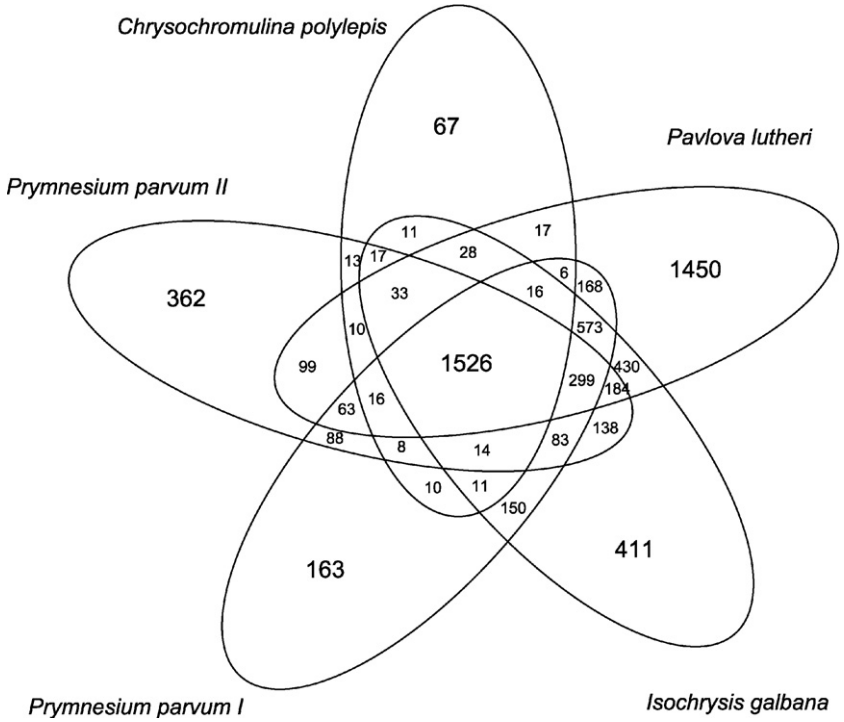

Fig. 1. Functional coverage comparisons of the haptophytes *I. galbana*, *C. polylepis*, *Pavlova lutheri*, *P. parvum I* (La Claire), *P. parvum II* (this work). Common and library-specific hit-distributions of transcripts to KOG/euNOG orthologies with an *e*-value of 10^{-10} or less are shown.

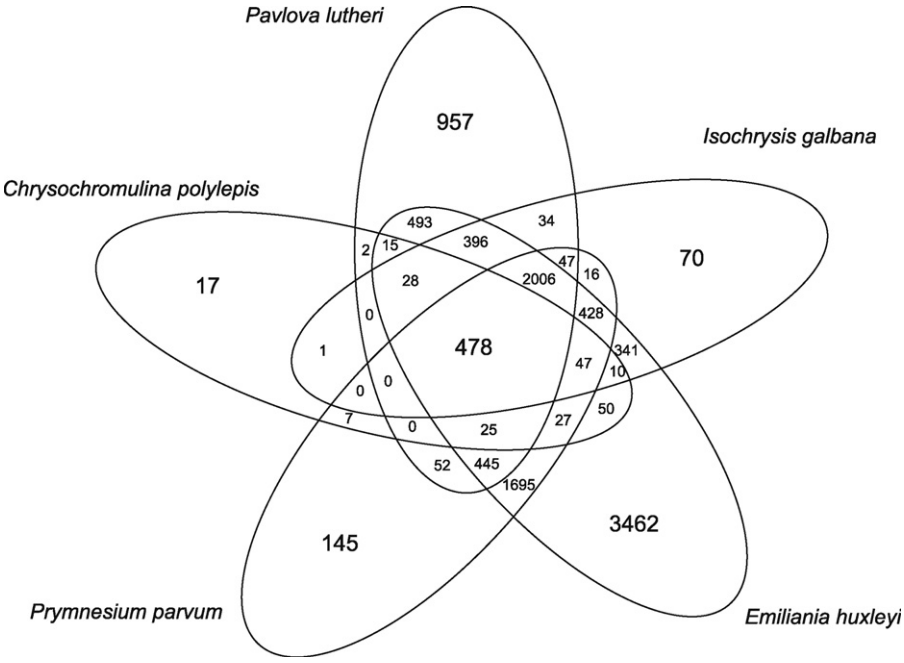

Fig. 2. Comparative analysis of KOG/eu NOG based functional annotated genes (*e*-value of 10^{-10} or less) in the haptophytes *I. galbana*, *C. polylepis*, *Pavlova lutheri*, *P. parvum* (EST libraries merged) in relation to the best transcript models from *E. huxleyi*.

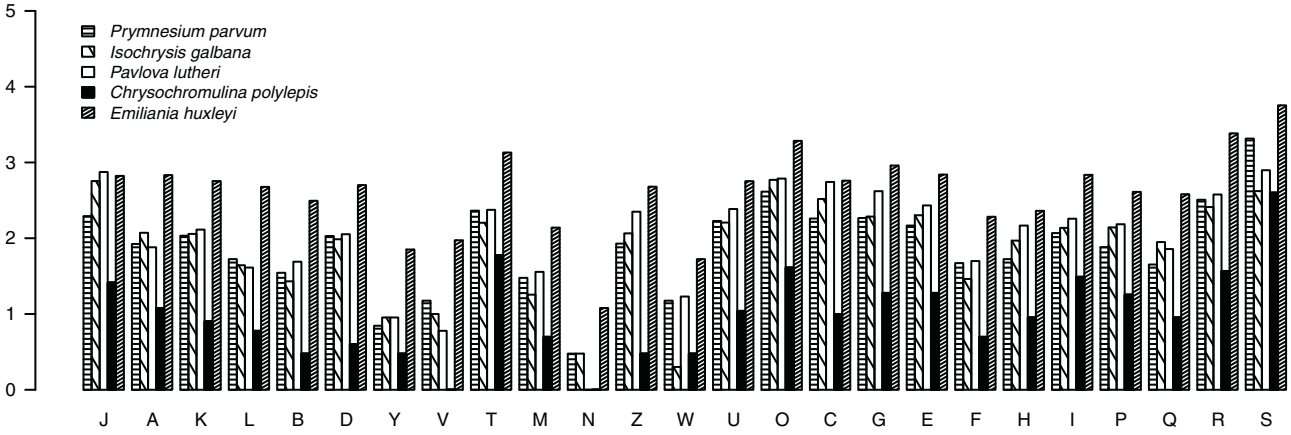

Fig. 3. Numbers of tentative unique genes with significant hits to KOG-categorized orthologies euNOG and KOG on a logarithmic scale. KOG categories (given as capital letters) are used to group the hit-counts of the respective library. (J – translation, ribosomal structure and biogenesis, A – RNA processing and modification, K – transcription, L – replication, recombination and repair, B – chromatin structure and dynamics, D – cell cycle control, cell division, chromosome partitioning, Y – nuclear structure, V – defence mechanisms, T – signal transduction, M – cell wall/membrane/envelope biogenesis, N – cell motility, Z – cytoskeleton, W – extracellular structures, U – intracellular trafficking, secretion, vesicular transport, O – posttranslational modification, protein turnover, chaperones, C – energy production and conversion, G – carbohydrate transport and metabolism, E – amino acid transport and metabolism, F – nucleotide transport and metabolism, H – coenzyme transport and metabolism, I – lipid transport and metabolism, P – inorganic ion transport and metabolism, Q – secondary metabolites biosynthesis, transport and catabolism, R – general function prediction only, S – function unknown.)

fragments showed significant hits to annotated genes based on similarity with an *e*-value below 10^{-10}. The best hits of more than half of the N- and P-relevant genes from the NCBI non-redundant database were to those of microalgal origin. Fourteen and six genes were found to be involved in the uptake, transport and storage of N and P, respectively. Tables 6 and 7 comprise a subset of nineteen genes involved in cell division and transcription, translation and vesicle transport, respectively.

3.2. Nutrient status of *Prymnesium parvum* cell cultures

The concentration of dissolved inorganic N and P (measured in the form of NO_2^-, NO_3^-, PO_4^{3-}) in the medium decreased with increasing cell concentration of the cultures (Fig. 4). At the first sampling point on Day 2, as the cells reached a concentration of about 5×10^4 ml^{-1}, the N- deprived cultures had used up about one third, whereas the N- and P-replete and P-deprived cells had consumed about ten percent of their original N resource. When the N-depleted cells reached stationary phase, the medium contained <0.5 μM NO_3^- and NO_2^-, whereas the consumption of PO_4^{3-} was not measurable. On the other hand, in the medium of the P-deprived cultures, an excess of NO_2^- and NO_3^- remained, but the final PO_4^{3-} concentration was <0.5 μM. The nutrient-replete control cultures used up almost all the N present in the form of NO_2^- and NO_3^-, but had an excess of available P measured as PO_4^{3-}. Surprisingly, the concentration of NH_4^+ in the medium

Table 5
Genes involved in acquisition, storage and transport of nitrogen and phosphorus in the EST library of *P. parvum*. Best hits from nr (non-redundant sequences database, GenBank) with *e*-values are shown, ↑ ↓ depicts up and downregulation, nd: no difference in gene expression in the exponential vs. stationary phase within treatment. Genes marked with asterisk have no expression data due to bad signal on the microarray.

TUGs in ESTTAL	Organism hit in nr	*e* value nr	Annotation	*e* value	Expression
Nitrogen assimilation					
44b11.m13f	*Chlamydomonas reinhardtii*	4E−08	KEGG: ammonium transporter	5.00E−05	P ↓
80g09.m13r	*Chlamydomonas reinhardtii*	5E−12	KEGG: probable high affinity ammonium transporter	2.00E−09	*
86e19.m13r	*Xenopus (Silurana) tropicalis*	6E−37	KOG: ammonium transporter	6.00E−37	P ↓
18c05.m13f	*Thalassiosira pseudonana*	1E−80	KEGG: formate/nitrite transporter	1.00E−46	nd
30f02.m23r	*Porphyra yezoensis*	5E−15	KEGG: high-affinity nitrate transporter, putative	2.00E−14	P ↓
88e12.m13f	*Prorocentrum minimum*	8E−32	KEGG: formate transporter	7.00E−23	R ↑
54h20.m13f	*Thalassiosira pseudonana*	1E−66	KEGG: formate/nitrite family of transporters	7.00E−39	P ↑
81a10.m13f	*Planctomyces maris*	6E−19	KEGG: glutamate synthase small subunit	2.00E−16	nd
07f04.m13r	*Chaetoceros compressus*	1E−60	KEGG: glnA; glutamine synthase	1.00E−34	nd
61b07.m13r	*Crocosphaera watsonii*	9E−23	KEGG: glutamine amidotransferas	1.00E−22	nd
58n22.m13f	*Thalassiosira pseudonana*	2E−42	KEGG: glutamine synthase	5.00E−25	nd
20e07.m13f	*Capsaspora owczarzaki*	2E−29	KOG: copper amine oxidase	4.00E−30	P ↓
Nitrogen storage					
16f03.m13r	*Thalassiosira pseudonana*	5E−31	KOG: aspartate aminotransferase	3.00E−23	nd
84g18.m13r	*Oryctolagus cuniculus*	1E−67	KOG: aspartate aminotransferase	6.00E−69	nd
47c10.m13r	*Thalassiosira pseudonana*	4E−33	KEGG: asparaginase [EC:3.5.1.1]	3.00E−22	nd
Phosphorus acquisition					
45e11.m13r	*Emiliania huxleyi*	8E−58	KEGG: phosphate-repressible phosphate permease	1.00E−24	P ↑, R ↓
46c04.m13r	*Schizosaccharomyces pombe*	3E−13	KEGG: probable inorganic phosphate transporter	4.00E−14	*
50e12.m13r	*Emiliania huxleyi virus 86*	1E−38	KEGG: putative phosphate/sulphate permease	6.00E−22	*
102j12.m13f	*Monosiga brevicollis*	1E−20	KOG: purple acid phosphatase	8.00E−11	P ↑
48g10.m13f	*Ectocarpus siliculosus*	6E−10	KEGG: phosphatidic acid phosphatase	4.00E−10	N, R ↑
55m11.m13r	*Aureococcus anophagefferens*	5E−49	KEGG: arsC; arsenate reductase	6.00E−21	R, N ↓, P ↑

Table 6
Selection of genes identified in the EST library, involved in cell proliferation, mitosis, meiosis, DNA/RNA transcription. Best hits from the nr (non-redundant sequences, GenBank) database are shown with BLAST alignment *e*-values. ↑ ↓ depicts up- and down-regulation, nd: no significant difference in gene expression in the exponential vs. stationary phase within treatment.

ID	nr hit	*e*-value nr	Best hit	*e*-value	Expression
89l02.m13f	*Pleurochrysis carterae*	1.00E−104	KEGG: proliferating cell nuclear antigen	4.00E−98	All ↓
56p15.m13f	*Physcomitrella patens*	7.00E−110	KEGG: replication factor	6.00E−108	All ↓
81e08.m13f	*Candida tropicalis*	2.00E−31	KEGG: replication factor	6.00E−32	nd
04a09.r1	*Chlorella variabilis*	2.00E−28	KOG: meiosis protein Mei2	6.00E−28	nd
64a09.m13r	*Nosema ceranae*	2.00E−11	KOG: meiosis protein Mei2	1.00E−12	nd
04h01.f1	*Nomascus leucog*	1.00E−11	KOG: DNA-dependent RNA polymerase	2.00E−13	nd
15h01.m13r	*Anolis carolinensis*	8.00E−44	KOG: DNA polymerase	1.00E−40	N, P ↓
102j06.m13r		2.00E−105	KOG: nucleosome remodeling protein	3.00E−107	P ↓
52n13.m13f	*Picea sitchensis*	8.00E−34	SP: DNA replication complex G	4.00E−30	All ↓
87l05.m13f	*Vigna aconitifolia*	6.00E−88	KEGG: similar to cell division protein	3.00E−88	All ↓
55a05.m13f	*Ectocarpus siliculosus*	3.00E−30	KEGG: cyclin-dependent kinases	1.00E−27	All ↓
101c18.m13r	*Physcomitrella patens*	1.00E−88	KEGG: RNA helicase	4.00E−51	All ↓
56p15.m13f	*Physcomitrella patens*	7.00E−110	KEGG: replication factor C subunit 3	6.00E−108	All ↓
89l02.m13f	*Pleurochrysis carterae*	1.00E−104	KEGG: proliferating cell nuclear antigen 2	4.00E−98	All ↓
97g10.m13f	*Selaginella moellendorffii*	4.00E−77	KOG: DNA polymerase delta	2.00E−72	All ↓
19f01.m13r	*Ectocarpus siliculosus*	2.00E−29	KEGG: POLA2; polymerase (DNA directed)	2.00E−25	All ↓

increased in both the nutrient-replete and P-depletion experiments, whereas it remained stable during developing N starvation.

3.3. Growth and toxicity of Prymnesium parvum

During early growth stages, the nutrient deprived cultures displayed similar growth and physiological characteristics to the nutrient replete controls. Cell concentrations increased exponentially until Day 4 after inoculation (Fig. 4). The N-deprived cultures stopped growing on Day 5, whereas the P-starved cells reached stationary phase on Day 10. The nutrient replete control cultures grew for eleven days and entered stationary phase at a cell concentration of about 1.3×10^6 cells ml^{-1}. The final concentrations of the starved cultures were lower (1.4×10^5 and 4.5×10^5 cells ml^{-1}, respectively, for the N- and P-starved cells). When the limiting nutrient was added, the cells resumed exponential growth in both N- and P-depleted cultures (Fig. 4), confirming that limitation by the corresponding nutrient was the cause of entering the stationary growth phase in the depleted cultures in a reversible manner.

In the early growth stages, the pH of all cultures increased similarly to about 8.5 by Day 4. On Day 5, the pH of the N-deprived cells decreased slightly, and in the following two days, it decreased to 8.2. In the P-deprived cultures, the pH increased further to 8.8 until Day 9 and then slowly decreased until Day 14 (to 8.5). The pH of the nutrient replete cultures, on the other hand, increased until Day 10 (reaching 9.55) and then decreased to 8.6 by Day 14 (Fig. 4).

The whole cell bioassay methods revealed the toxicity of *P. parvum* cells with respect to both allelopathic capacity and intracellular toxicity. Generally, no difference in allelopathic capacity measured with the *Rhodomonas* bioassay was observed in the early- and mid-exponential growth phase among the

Table 7
Selected genes identified in the EST library involved in vesicle transport, secretion and mixotrophy. Best hits from nr (non-redundant sequences, GenBank) database are shown with *e*-value. ↑ ↓ depicts up and downregulation, nd: no significant difference in gene expression in the exponential vs. stationary phase within treatment.

ID	Best hit nr	*e*-value (nr)	Best hit	*e*-value	Expression
59a12.m13f	*Naegleria gruberi*	8.00E−17	KOG: vacuolar protein sorting assiciated protein	3.00E−15	N ↑
41i06.m13f	*Drosophila virilis*	3.00E−30	KOG: multidrug resistance-associated protein	9.00E−31	N, C ↑
97k06.m13f	*Picea sitchensis*	4.00E−76	KOG: protein required for fusion of vesicles	7.00E−70	P ↑
90b10.m13f	*Ostreococcus lucimarinus*	1.00E−27	KOG: GTP-binding ADP-ribosylation factor	8.00E−29	P ↑
98n14.m13f	*Bos taurus*	2E−101	KEGG: dynein, axonema	2.00E−100	N ↑
41k04.m13f	*Chlamydomonas incerta*	2.00E−33	KOG: microtubule-associated anchor protein	7.00E−34	P ↑
102p20.m13f	*Thalassiosira pseudonana*	6.00E−38	KEGG: hemolysin III	1.00E−25	nd
04d12.fm13f	*Selaginella moellendorffii*	3.00E−13	KOG: SNARE protein SED5/S	1.00E−12	nd
09h07.m13f	*Ricinus communis*	5.00E−33	KOG: importin	2.00E−32	nd
73g12.m13r	*Ailuropoda melanoleuca*	8.00E−46	KEGG: karyopherin (importin)	1.00E−46	P ↓
78f04.m13f	*Sorghum bicolor*	4.00E−45	KOG: karyopherin (importin)	2.00E−43	nd
94a10.m13r	*Populus trichocarpa*	2.00E−44	KEGG: exportin	2.00E−43	nd
95k15.m13f	*Chlorella variabilis*	1.00E−68	KEGG: karyopherin alpha	6.00E−64	nd
18g09.m13r	*Aureococcus anophagefferens*	2.00E−60	KOG: clathrin adaptor complex	1.00E−57	nd
21b07.m13f	*Micromonas pusilla*	3.00E−22	KEGG: clathrin, heavy polypeptide	4.00E−20	nd
21f10.m13r	*Capsaspora owczarzaki*	9.00E−25	KOG: vesicle coat complex	9.00E−24	nd
73f11.m13r	*Branchiostoma floridae*	5.00E−36	KOG: clathrin coat dissociation kinase	4.00E−36	nd
mixotrophy					
41k04.m13f	*Chlamydomonas incerta*	2.00E−33	KEGG: autophagy related protein	5.00E−33	P ↑
72j24.m13r	*Ectocarpus siliculosus*	1.00E−44	SP: autophagy-related protein 18	3.00E−44	nd

treatments. At the first sampling point (early exponential growth), extracellular toxicity was not very pronounced. The undiluted samples caused about 40% lysis of *Rhodomonas* cells, irrespective of treatment; the EC_{50} values were estimated at around 10^5. Similarly, at the second sampling point, there was no significant difference in the extracellular toxicity of nutrient deprived versus replete cells. Again, the EC_{50} value was close to 10^5 for all treatments (Fig. 5). However, toxicity in the stationary phase differed markedly among the three treatments. The nutrient replete cultures grew to cell concentrations beyond 10^6 ml^{-1} and the allelopathic capacity decreased (EC_{50} values rose to between 6 and 8×10^5). The N-depleted cells showed a similar decrease in toxicity, whereas the extracellular toxicity of the P-starved cells remained unaltered in the stationary phase.

The fish erythrocyte test was applied to assess the intracellular toxicity of nutrient-deprived and replete *P. parvum* cells (Fig. 6). The intracellular toxicity remained unchanged throughout the growth phase in the case of N-deprived cells, whereas it decreased in nutrient replete cultures in stationary phase. On the other hand, P-starvation greatly enhanced the intracellular toxicity in *P. parvum*. A two-way ANOVA test indicated that only treatment (nutrient replete or deprived) had a significant effect on intracellular toxicity at $p = 0.95$, but not the growth phase (exponential or stationary). Subsequent pairwise *t* tests with a

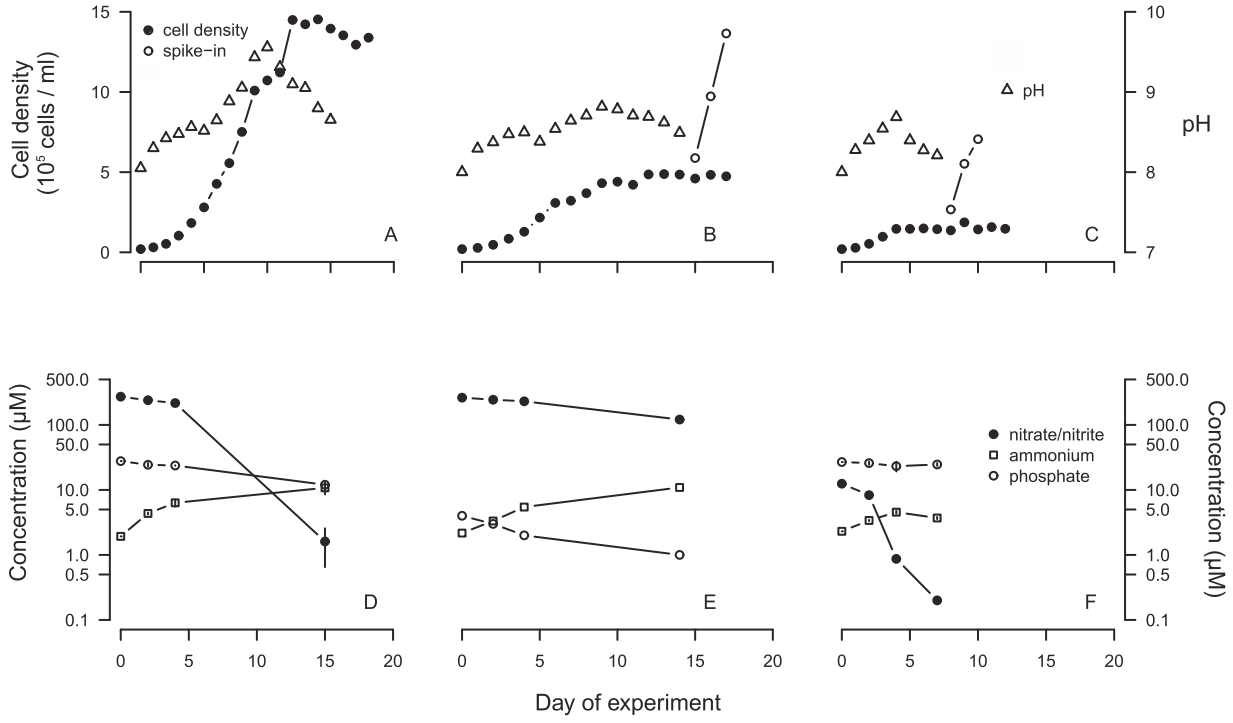

Fig. 4. Growth, pH and dissolved nutrient concentrations of *P. parvum* batch cultures throughout the experiments. (A–C) Daily cell concentration measurements (in 10^5 cells/ml; solid and empty circles; common *Y* axis on left hand side) and the pH of the cultures (triangles; common *Y* axis on right hand side); (D–F) dissolved nutrient concentrations in the early exponential, mid exponential and stationary growth phases on a logarithmic scale (in µM). Treatments: (A and D) nutrient replete control; (B and E) phosphate depletion; (C and F) nitrate depletion. Subplots in the same rows and columns are scaled identically on their *Y* and *X* axes, respectively. *X* axes: time in days.

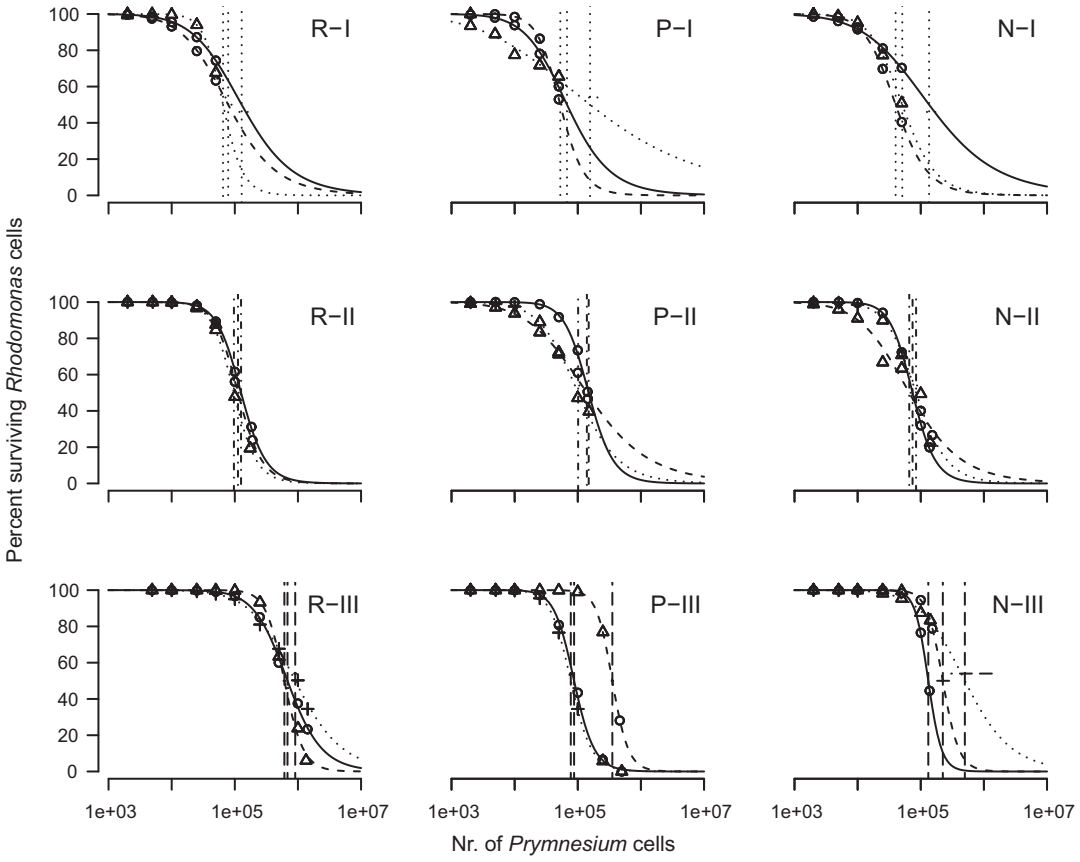

Fig. 5. Extracellular toxicity of *Prymnesium parvum* against the cryptomonad *Rhodomonas salina* under different treatments and growth phases. Estimated survival proportions (symbols) and posterior median dose-response curves fitted to *Rhodomonas salina* survival data as function of *Prymnesium parvum* cell concentration using a Bayesian approach. Treatments: first column: (R) nutrient replete control; second column: (P) phosphate depletion; third column: (N) nitrate depletion. Growth phases: first row: (I) early exponential; second row: (II) mid-exponential; (III) third row: stationary phase. *X* axes: number of *P. parvum* cells inoculated; *Y* axes: estimated proportion of surviving *R. salina* cells (percent). Vertical lines represent the posterior median of EC50, and horizontal lines at 50% height represent the 95% highest posterior density interval of EC50. The three curves represent the three replicates on each panel.

Benjamini–Hochberg correction for multiple testing among treatments indicated a significant difference of the phosphate depleted cultures from the other two (corrected *p* values: 0.000093 and 0.00093 when compared with the control and nitrogen starvation, respectively), whereas the differences between control and nitrogen starvation were not significant.

3.4. Gene expression pattern analysis with microarrays

Of the approximately 6300 sequences in our data set, 1742 were identified as differentially expressed between at least one combination of the three physiological growth phases of the nutrient replete or deprived cultures. When searching for growth dependent gene expression patterns, we found the highest number of differentially expressed genes when comparing cells in early exponential versus stationary growth phases. There was a much

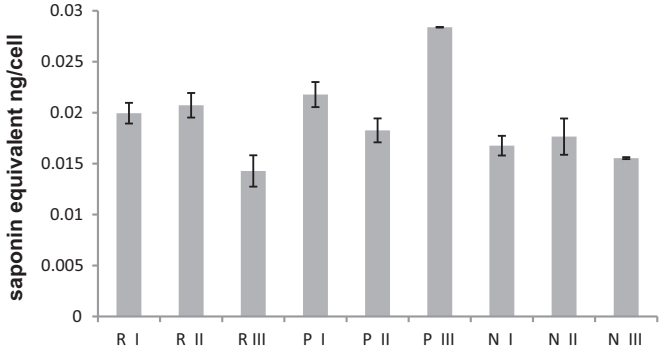

Fig. 6. Intracellular toxicity of *P. parvum* given in nanogram saponin equivalent per cell, average of biological triplicates; with standard deviation shown. *X* axis: treatments (R – nutrient replete control; P – phosphate depletion; N – nitrate depletion; growth phases: I – early exponential; II – mid-exponential; III – stationary phase).

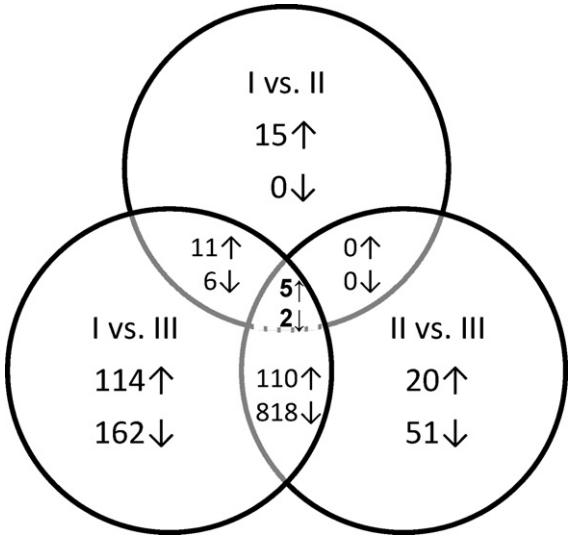

Fig. 7. Growth phase dependent gene expression of *P. parvum*. ↑ ↓ depicts up and downregulation of genes between different growth phases irrespective of treatment. Growth phases: I – early exponential; II – mid-exponential; III – stationary phase.

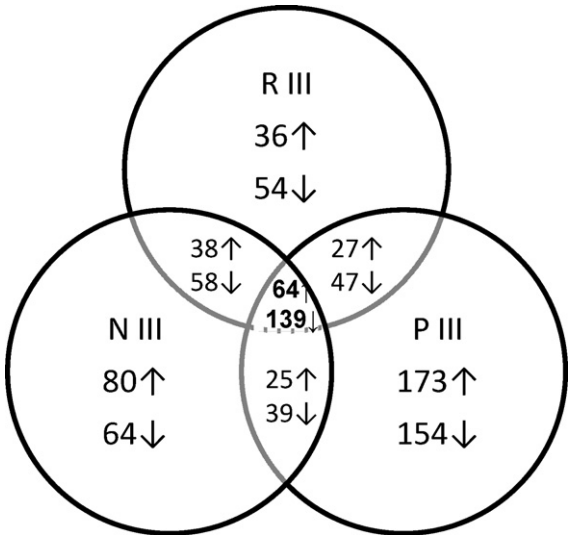

Fig. 8. Treatment specific gene expression differences in *P. parvum*. Numbers of genes differentially regulated in the stationary phase of nitrogen depleted (NIII), phosphorus depleted (PIII) and replete control (RIII) cultures. ↑ ↓ depicts up- and down-regulation of genes between starved and replete stationary cells.

smaller difference observed in expression patterns when comparing the two exponential phases or the mid-exponential with stationary phase (Fig. 7).

We observed the up- and down-regulation of 64 and 139 genes, respectively, in all stationary phase cells as compared to the early exponential phase within treatments (Fig. 8). Unfortunately, but as expected, no annotation could be assigned to the vast majority of the upregulated genes. Interestingly, two bicarbonate transporter genes were identified among the ESTs and both were found to be upregulated. One fragment showed elevated expression in all treatments, approximately six-fold in the deprived versus 14-fold in the replete stationary phase cells, whereas expression of the other fragment was elevated only in the N-depleted and nutrient replete cultures, at six and 14-fold upregulation, respectively. Among the downregulated genes, we found those involved in cell division, mitosis, DNA/RNA transcription, translation, photosynthesis (Table 6). The expression of the genes putatively involved in vesicle transport and secretion showed also a growth-phase dependent pattern (Table 7). Almost all genes that exhibited differential expression were upregulated in the stationary phase of nutrient depleted cells.

In total 327 genes were differentially expressed only in the P-deprivation treatment, with 173 genes uniquely up- and 154 down-regulated in the P-limited stationary phase cells. Among the upregulated genes, we identified specific responses, such as the elevated mRNA concentration of a phosphate repressible phosphate permease (40-fold increase), and acid phosphatase (13-fold increase), an arsenate reductase (4.6-fold increase) and a triose phosphate/phosphate translocator (4-fold increase) (Table 5). Among downregulated genes, we observed reduced expression levels of translation initiation factors and ribosomal proteins, and of many unknown genes, only under P-starvation.

In the stationary growth phase of the N-depletion experiment, 80 genes were uniquely upregulated, whereas 64 were down-regulated as compared to the exponential phase. No function could be assigned to the majority of the upregulated genes. No upregulation of any genes putatively involved in acclimation to N-starvation (Table 5) was observed. Nevertheless, some genes such as a Photosystem II stability/assembly factor, nuclear transportation factor, and an actin regulating protein were downregulated in the N-starved stationary phase cells.

4. Discussion

4.1. Comparison of EST libraries for prymnesiophytes

The normalized EST library of the toxic prymnesiophyte *P. parvum* includes genes expressed in a variety of physiological states induced under a variety of environmental regimes. Alteration of nutrient concentrations and ratios along the growth curve provided significant insights into the transcriptome of this toxic species. Comparison with several EST datasets available for prymnesiophytes, including the non-toxic *I. galbana* (Patron et al., 2006), *P. lutheri* (Patron et al., 2006) and *E. huxleyi*, and the toxic species *C. polylepis* (John et al., 2010), serves to distinguish gene functions common to prymnesiophytes from toxin-specific elements. Our comparison of the two *P. parvum* libraries, based on their functional annotation, almost doubled the number of KEGG metabolic enzymes identified from this species as compared with those identified in the EST library constructed by La Claire (2006) (Table 2). This highlights the importance of sampling RNA species over a wide range of environmental regimes. In any case, when comparing *P. parvum* genes to other prymnesiophyte sequences, we observed a distribution of functional categories similar to that in non-toxic *P. lutheri* and *I. galbana* (Fig. 3). On the one hand, the categories 'defence mechanisms' (V) and 'function unknown' (S) appear to be overrepresented in the *P. parvum* libraries. On the other hand, in the category 'translation, ribosomal structures and biogenesis' (J) less hits were found in the libraries of *P. parvum* than in the other species. This phenomenon is probably due to the fact that our EST library was normalized, whereas those of *I. galbana* and *P. lutheri* were not, thus enabling us to catch more of the "gene space".

4.2. Nutrient effects on toxicity and gene expression

4.2.1. Effect of phosphorus starvation

The allelopathic capacity or extracellular toxicity of *P. parvum* against different organisms, including the brine shrimp *Artemia salina* (Graneli and Johansson, 2003; Larsen and Bryant, 1998; Larsen et al., 1993; Meldahl et al., 1995), the cryptomonad *Rhodomonas baltica/salina*: (Barreiro et al., 2005; Skovgaard and Hansen, 2003), and fish (*Pimemphales promelas*) (Baker et al., 2007; Henrikson et al., 2010; Schug et al., 2010; Valenti et al., 2010) has been monitored in many studies. In a consistent pattern, the extra- and intracellular toxicity of P-starved cells has been elevated in comparison to P-replete cells (Graneli and Johansson, 2003; Johansson and Granéli, 1999; Uronen et al., 2005). In accord, we also found enhanced overall toxicity in the stationary phase of the P-starved cells.

In addition to the shift up in toxicity, we also found a marked transcriptional response to P-starvation. The upregulated phosphate-repressible phosphate permease (Table 5) shows high similarity to a such permease from *E. huxleyi* (Table 5), the expression of which also increases under P-starvation (Dyhrman et al., 2006). Our finding is also in accordance with the observations of upregulation of three different phosphate transporter genes in phosphate-depleted *Chlamydomonas reinhardtii* cells (Moseley et al., 2006). Furthermore, a phosphate transporter gene (TcPHO) from the prasinophyte *Tetraselmis chui* was found to be upregulated in P starved cells (Chung et al., 2003). In *Chlorella*, *E. huxleyi* and *Chlamydomonas*, the expression of acid phosphatases and phosphohydrolases was elevated under low nutrient concentrations, but more so under N depletion than under P limitation (Abel et al., 2002; Kruskopf and Du Plessis, 2004; Riegman et al., 2000; Ticconi and Abel, 2004). These enzymes either hydrolize phosphate esters to access extracellular, organically bound phosphate nutrients under acidic conditions, or they are involved in intracellular relocation of phosphate.

High intracellular levels of phosphorus are required for various chloroplast functions. In *Chlamydomonas*, phosphate is transported from the cytosol into the chloroplast, where it is incorporated into starch bodies. Translocators of phosphate/triose or hexose phosphate are activated when P is limiting (Sharkey et al., 2004). In our experiment with *P. parvum*, the expression of a putative glucose-6-phosphate/phosphate or phosphoenolpyruvate/phosphate antiporter occurred even in the P starved cells during all culture phases. However, the expression of the same gene was reduced in the stationary nutrient-replete and N-depleted cells.

Interestingly, two fragments showing high similarity to genes encoded by the arsenic detoxification operon in bacteria were identified in our EST library. The arsH gene with unknown function was upregulated five-fold during P-starvation. The arsC gene has been shown to be an arsenate reductase required for arsenate detoxification in *Sinorhizobium meliloti* (Yang et al., 2005). The expression of this gene in *P. parvum* remained unaltered in the P-starvation experiment, whereas it was downregulated in the stationary phase of the N starved and the nutrient replete stationary cells. In the diatom *Skeletonema costatum* increasing concentration of arsenate causes elevated uptake, whereas increased phosphate concentrations cause decreased arsenate uptake rates. Arsenic concentrations in cells grown at relatively high P concentration were an order of magnitude lower than in cells grown under P limited conditions (Sanders and Windom, 1980). These authors concluded that since arsenate is a chemical analogue of phosphate, arsenate and phosphate compete for uptake by algal cells. Although we do not know the amount of arsenic in the seawater used in the experiment, we assume that under P-limiting conditions elevated arsenate uptake took place, which in turn caused elevated expression of the arsenic detoxification genes.

These findings suggest that *P. parvum* reacts to P limitation specifically on the gene expression level, a strategy also known to be applied by other microalgae (Dyhrman et al., 2006; Wurch et al., 2011).

4.2.2. Nitrogen starvation

Several researchers found enhanced intracellular toxicity in N-starved *P. parvum* cells (Johansson and Granéli, 1999; Uronen et al., 2005), but according to others, the toxicity of N-depleted cells does not differ significantly from that of nutrient replete cells (Lindehoff et al., 2009; Sopanen et al., 2008). Our findings concerning the intracellular toxicity support the latter observation (Fig. 6). Furthermore, the allelopathic capacity as reflected in the extracellular toxicity of N-starved *P. parvum* cells remained unchanged throughout in all culture phases. The allelochemical activity did not differ from that of the nutrient supplied cultures for the first two sampling points, whereas a decrease was observed for stationary phase nutrient-replete cells (Fig. 5).

The microarray approach served to illustrate the effect of N-starvation on the gene expression pattern of *P. parvum*. Similar gene expression studies have been performed with the pelagophyte *Aureococcus anophagefferens* (Wurch et al., 2011), the dinoflagellate *A. minutum* (Yang et al., 2011) and the haptophyte *E. huxleyi* (Dyhrman et al., 2006). These latter authors applied long serial analysis of gene expression (SAGE) to study the effect of N-depletion on *E. huxleyi*. They identified 38 genes upregulated under N-starvation, but no function could be assigned to most of them. In our study 80 genes were uniquely up- and 64 down-regulated in the N-starved stationary cells. We were not able to assign function based on sequence similarity to the majority of the upregulated genes. Surprisingly, no clear N-starvation response was discernable on the gene expression level, because none of the genes putatively involved in N acquisition, transportation and storage were upregulated under N-starvation. In contrast to *P. parvum*, the non-toxic and presumably non-mixotroph haptophyte *I. galbana*, reacts to N-starvation by up-regulation of nitrate and ammonium transporters (Kang et al., 2007, 2009). In this case, an increase of mRNA level of both transporter genes was observed in N-depleted, to nitrate conditioned cells of *I. galbana*, but when ammonium and nitrate was provided, the expression of both transporter genes decreased. Moreover, the expression of a glutamine synthase gene in *I. galbana* was upregulated in nitrogen depleted cells, whereas no differential regulation was shown in the presence of ammonium (Kang et al., 2007).

P. parvum was shown to possess cell surface L-amino acid oxidase(s), which oxidize amino acids and amines from organic matter, liberating ammonium, which is subsequently taken up by the cells (Palenik and Morel, 1991). No amine oxidase enzyme activity was found by these authors in the presence of ammonium, whereas nitrate and N-starvation triggered higher enzyme activity (Palenik and Morel, 1991). In agreement with this observation, a copper dependent amine oxidase (Table 5) was identified from *P. parvum*. It was down-regulated in P-depleted stationary cells, whereas no difference in the gene expression was observed in N-depleted and nutrient replete stationary phase cells.

We observed increasing extracellular ammonium levels under all treatments as the cell concentrations increased in cultures. The highest amount was measured in the stationary phase nutrient-replete and depleted cultures, and even N-depleted cells liberated some ammonium.

This phenomenon may be due to increased amine oxidase activity with growth under low nitrate levels in the medium. Alternatively, ammonium could have leaked from disintegrating cells under all treatments. Potential bacterial contribution to ammonium recycling is assumed to be negligible because they were largely absent from the growth medium. In any case, the collective evidence suggests that *P. parvum* does not react to N-starvation as other microalgae, namely with elevated expression of genes involved in the acquisition, transportation and storage of N.

A marked decrease was observed in the expression of cytochrome and light-harvesting related genes under all treatments in the stationary growth phase. In N-starved cells it may be a treatment-specific response, given the high N-dependency of photosynthesis, e.g. for the biosynthesis of chlorophyll and photosynthesis associated proteins. Indeed, the shortage on N generally results in lower amount of chlorophyll per cell in algae (de Groot et al., 2003). Gene expression analyses of microalgae also support this finding ((Dyhrman et al., 2006; Yang et al., 2011). Due to low photosynthetic capacity of the cells, increased amount of reactive oxygen species are often observed. In accordance with these findings, the expression of an alternative oxidase was found unaltered in N starved cells, whereas its expression decreased in replete or P starved stationary cells.

4.2.3. Phagotrophy

Stoecker (1998) developed conceptual models for the classification of mixotroph planktonic protists, based on their response to environmental conditions (such as availability of light, nutrients etc.). Under this scheme, *P. parvum* belongs in Category IIA (phagotrophic "algae"), comprising primarily photosynthetic species, that are able to assimilate inorganic nutrients. The phagotrophic feeding in the members of this group is typically triggered by limiting inorganic nutrients.

Elevated prey feeding frequency under macronutrient starvation has been observed frequently in *P. parvum* (Carvalho and Granéli, 2010; Legrand et al., 2001; Nygaard and Tobiesen, 1993). On this basis, it has been estimated that approximately 70% of the cellular N content in N deficient and 36% of cellular P in P-starved *Prymnesium* cells originated from prey organisms (Carvalho and

Granéli, 2010). However, some feeding was also observed in nutrient sufficient *Prymnesium* cultures, contributing to about 30% of the cellular amount of either macronutrient (Carvalho and Granéli, 2010), suggesting that phagotrophy is an adaptive strategy of this species (Carvalho and Granéli, 2010). Accordingly, during our experiments the highest amount of feeding activity likely occurred in the N-limited cultures. *Prymnesium* was grown in unialgal batch cultures where bacteria were largely absent, therefore we postulate that active cells fed on debris originating from disintegrating cells, or cannibalistically on weak *P. parvum* cells, a behaviour that has been observed previously and only to a lesser extent on bacteria (Nygaard and Tobiesen, 1993; Skovgaard and Hansen, 2003).

Sillo and co-workers identified more than 400 genes that are differentially regulated in the slime mold *Dictyostelium* by phagocytosis (Sillo et al., 2008). However, the vast majority of these genes could not be annotated based on similarity, and only a few could be identified as coding for proteins possibly involved in phagocytosis. Among such genes are fragments related to cell adhesion, receptor proteins, or are involved in vesicle transport (Sillo et al., 2008). We identified in our EST library several fragments putatively involved in vesicle transport and secretion such as autophagy related proteins, exportin/importin fragments, clathrin and vesicle coat proteins (Table 6). The up-regulation of genes (depicted in Table 7) putatively involved in vesicle transport and secretion could be related to enhanced toxicity of stationary cells, or else it may be due to higher frequency of phagotrophy, specifically cannibalistic feeding on disintegrated cells. Given that *P. parvum* is a mixotrophic species capable of particle uptake, we speculate that at least some of the unknown genes upregulated under N-deficiency may be involved in heterotrophic nutrition of this species.

4.2.4. Genes expressed in the different growth phases

A high number of genes were regulated in a growth phase-linked manner. Altogether 64 and 139 genes were up and down-regulated in stationary phase as compared to exponentially growing cells. The gene expression pattern differed more in a growth-phase dependent manner, than among different treatments at the same physiological state. We could not assign any function to most of the genes upregulated in the stationary growth phase cells under all treatments. This is not surprising, considering that the functional identification of these genes is achieved only through similarity comparisons. Still, the general pattern of overall decrease in the expression of genes involved in photosynthesis, cell proliferation, and signal transduction demonstrated the reduced cellular anabolic processes in stationary phase cells. Interestingly, a bicarbonate transporter was upregulated to a different extent among all treatments. Highest up-regulation was observed in stationary phase nutrient-replete cultures, where the pH of the medium reached up to 9. Such a high pH is a common phenomenon in natural blooms where during dense *P. parvum* blooms the pH can even exceed 9 (Lindholm and Virtanen, 1992; Michaloudi et al., 2009). As photosynthetic cells grow and increase in concentration the pH of the medium increases in a closed system (e.g. batch culture) because the algae use up the dissolved carbon in the medium (Fig. 4). At pH 8–9, bicarbonate ion is the predominant carbon species in the medium, and as the concentration of dissolved carbon in the medium decreases, the expression of the bicarbonate transporter increases in order to compensate for carbon depletion and support higher rates of uptake. In aerated cultures (such as used in this study), the pH of the medium decreases slowly in the stationary growth phase, due to the inflow of fresh CO_2, reduced rate of photosynthesis and respiration of the senescent algal cells.

5. Conclusions

A normalized EST library was constructed and served as a genetic basis for gene expression studies of the toxic prymnesiophyte *P. parvum*. We monitored the physiological and gene expression responses of *P. parvum* to low N or P levels. We observed an overall higher toxicity under P-starvation, but not under N-limitation, as compared to nutrient replete cells. Furthermore, genes involved in the transport, mobilization and intracellular relocation of P were identified and found to be upregulated in P-starved cells. Several identified genes are involved in the acquisition and storage of N, but in contrast to the standard model in prymnesiophytes and most other photosynthetic protists these were not differentially regulated under N-starvation. Still, many unknown genes showed elevated corresponding mRNA levels in N-limited cells. *P. parvum* reacted to P-limitation on the gene expression level by up-regulating genes involved in the acquisition and transport of P. Since no such reaction to N starvation was detected, *Prymnesium* is obviously able to compensate for the shortage of inorganic N by other mechanisms, possibly by elevated heterotrophic activity such as phagotrophy upon debris and senescent cells.

We propose that the genes upregulated in N- or P-deprived cells can be used as sensitive biomarkers of nutrient physiological status in cultures and natural blooms of prymnesiophytes and also as indicators for potential bloom events.

Acknowledgements

This research was supported as part of the Sixth Framework EU project ESTTAL (GOCE-CT2004-511154). We thank AWI co-workers Bánk Beszteri for analysis of the allelopathic assay data and Klaus Valentin for helpful discussion regarding the molecular data set. We also gratefully acknowledge the contribution of the CeBiTec platform for oligonucleotide design.[SS]

References

Abel, S., Ticconi, C., Delatorre, C.A., 2002. Phosphate sensing in higher plants. Physiologia Plantarum 115, 1–8.

Alizadeh, A.A., Eisen, M.B., Davis, R.E., Ma, C., Lossos, I.S., Rosenwald, A., Boldrick, J.C., Sabet, H., Tran, T., Yu, X., Powell, J.I., Yang, L., Marti, G.E., Moore, T., Hudson, J., Lu, L., Lewis, D.B., Tibshirani, R., Sherlock, G., Chan, W.C., Greiner, T.C., Weisenburger, D.D., Armitage, J.O., Warnke, R., Levy, R., Wilson, W., Grever, M.R., Byrd, J.C., Botstein, D., Brown, P.O., Staudt, L.M., 2000. Distinct types of diffuse large B-cell lymphoma identified by gene expression profiling. Nature 403 (6769), 503–511.

Altschul, S.F., Madden, T.L., Schäffer, A.A., Zhang, J., Zhang, Z., Miller, W., Lipman, D.J., 1997. Gapped BLAST and PSI-BLAST: a new generation of protein database search programs. Nucleic Acids Research 25 (17), 3389–3402.

Baker, J.W., Grover, J.P., Brooks, B.W., Ureña-Boeck, F., Roelke, D.L., Errera, R., Kiesling, R.L., 2007. Growth and toxicity of *Prymnesium parvum* (Haptophyta) as a function of salinity, light and temperature. Journal of Phycology 43 (2), 219–227.

Barreiro, A., Guisande, C., Maneiro, I., Lien, T.P., Legrand, C., Tamminen, T., Lehtinen, S., Uronen, P., Granéli, E., 2005. Relative importance of the different negative effects of the toxic haptophyte *Prymnesium parvum* on *Rhodomonas salina* and *Brachionus plicatilis*. Aquatic Microbial Ecology 38 (3), 259–267.

Brown, K.L., Twing, K.I., Robertson, D.L., 2009. Unraveling the regulation of nitrogen assimilation in the marine diatom *Thalassiosira pseudonana* (Bacillariophyceae): diurnal variations in transcript levels for five genes involved in nitrogen assimilation. Journal of Phycology 45 (2), 413–426.

Bruhn, A., LaRoche, J., Richardson, K., 2010. *Emiliania huxleyi* (Prymnesiophyceae): nitrogen-metabolism genes and their expression in response to external nitrogen sources. Journal of Phycology 46 (2), 266–277.

Carvalho, W.F., Granéli, E., 2010. Contribution of phagotrophy versus autotrophy to *Prymnesium parvum* growth under nitrogen and phosphorus sufficiency and deficiency. Harmful Algae 9 (1), 105–115.

Chung, C.-C., Hwang, S.-P.L., Chang, J., 2003. Identification of a high-affinity phosphate transporter gene in a prasinophyte alga, *Tetraselmis chui*, and its expression under nutrient limitation. Applied and Environment Microbiology 69 (2), 754–759.

de Groot, C.C., van den Boogaard, R., Marcelis, L.F.M., Harbinson, J., Lambers, H., 2003. Contrasting effects of N and P deprivation on the regulation of photosynthesis in tomato plants in relation to feedback limitation. Journal of Experimental Botany 54 (389), 1957–1967.

Dyhrman, S.T., Haley, S.T., Birkeland, S.R., Wurch, L.L., Cipriano, M.J., McArthur, A.G., 2006. Long serial analysis of gene expression for gene discovery and transcriptome profiling in the widespread marine coccolithophore *Emiliania huxleyi*. Applied and Environmental Microbiology 72 (1), 252–260.

Eddy, S.R., 1998. Profile hidden Markov models. Bioinformatics 14 (9), 755–763.

Edvardsen, B., Imai, I., 2006. The Ecology of Harmful Flagellates Within Prymnesiophyceae and Raphidophyceae. In: Granéli, E., Turner, J.T. (Eds.), Ecology of Harmful Algae. Springer, Berlin Heidelberg, pp. 67–79.

Edvardsen, B., Paasche, E., 1998. Bloom dynamics and physiology of *Prymnesium* and *Chrysochromulina*. In: Anderson, D.M., Cembella, A.D., Hallegraeff, G.M. (Eds.), Physiological Ecology of Harmful Algae Blooms. Springer Verlag, Belin/Heidelberg/New York, pp. 193–208.

Eppley, R.W., Holmes, R.W., Strickland, J.D.H., 1967. Sinking rates of marine phytoplankton measured with a fluorometer. Journal of Experimental Marine Biology and Ecology 1, 191–208.

Eschbach, E., John, U., Reckermann, M., Cembella, A.D., Edvardsen, B., Medlin, L.K., 2005. Cell cycle dependent expression of toxicity by the ichthyotoxic prymnesiophyte *Chrysochromulina polylepis*. Aquatic Microbial Ecology 39, 85–95.

Eschbach, E., Scharsack, J., John, U., Medlin, L.K., 2001. Improved erythrocyte lysis assay in microtitre plates for sensitive detection and efficient measurement of haemolytic compounds from ichthyotoxic algae. Journal of Applied Toxicology 21 (6), 513–519.

Fistarol, G.O., Legrand, C., Graneli, E., 2003. Allelopathic effect of *Prymnesium parvum* on a natural plankton community. Marine Ecology Progress Series 255, 115–125.

Freitag, M., Beszteri, S., Vogel, H., John, U., 2011. Effects of physiological shock treatments on toxicity and polyketide synthase gene expression in *Prymnesium parvum* (Prymnesiophyceae). European Journal of Phycology 46 (3), 193–201.

Graneli, E., Johansson, N., 2003. Increase in the production of allelopathic substances by *Prymnesium parvum* cells grown under N- or P-deficient conditions. Harmful Algae 2 (2), 135–145.

Granéli, E., Salomon, P.S., 2010. Factors influencing allelopathy and toxicity in *Prymnesium parvum*. JAWRA Journal of the American Water Resources Association 46 (1), 108–120.

Henrikson, J.C., Gharfeh, M.S., Easton, A.C., Easton, J.D., Glenn, K.L., Shadfan, M., Mooberry, S.L., Hambright, K.D., Cichewicz, R.H., 2010. Reassessing the ichthyotoxin profile of cultured *Prymnesium parvum* (golden algae) and comparing it to samples collected from recent freshwater bloom and fish kill events in North America. Toxicon 55 (7), 1396–1404.

Hobbie, J.E., Daley, R.J., Jasper, S., 1977. Use of nuclepore filters for counting bacteria by fluorescence microscopy. Applied and Environmental Microbiology 33, 1225–1228.

Igarashi, T., Satake, M., Yasumoto, T., 1999. Structural and partial sterochemical assignments for prymnesin-1 and prymnesin-2: potent hemolytic and ichtyotoxic glycosides isolated from the red tide alga *Prymnesium parvum*. Journal of the American Chemical Society 121, 8499–8511.

Johansson, N., Granéli, E., 1999. Influence of different nutrient conditions on cell density, chemical composition and toxicity of *Prymnesium parvum* (Haptophyta) in semi-continuous cultures. Journal of Experimental Marine Biology and Ecology 239 (2), 243–258.

John, U., Beszteri, S.G.G., Singh, R., Medlin, L., Cembella, A.D., 2010. Genomic characterisation of the ichthyotoxic prymnesiophyte *Chrysochromulina polylepis*, and the expression of polyketide synthase genes in synchronized cultures. European Journal of Phycology 45 (3), 215–229.

John, U., Tillmann, U., Medlin, L., 2002. A comparative approach to study inhibition of grazing and lipid composition of a toxic and non-toxic clone of *Chrysochromulina polylepis* (Prymnesiophyceae). Harmful Algae 1, 45–57.

Kaartvedt, S., Johnsen, T.M., Aksnes, D.L., Lie, U., Svendsen, H.S., 1991. Occurence of the toxic phytoflagellate *Prymnesium parvum* and associated fish mortality in a Norwegian fjord system. Canadian Journal of Fisheries and Aquatic Sciences 48, 2316–2323.

Kang, L.-K., Hwang, S.-P.L., Gong, G.-C., Lin, H.-J., Chen, P.-C., Chang, J., 2007. Influences of nitrogen deficiency on the transcript levels of ammonium transporter, nitrate transporter and glutamine synthetase genes in *Isochrysis galbana* (Isochrysidales, Haptophyta). Phycologia 46 (5), 521–533.

Kang, L.-K., Hwang, S.-P.L., Lin, H.-J., Chen, P.-C., Chang, J., 2009. Establishment of minimal and maximal transcript levels for nitrate transporter genes for detecting nitrogen deficiency in the marine phytoplankton *Isochrysis galbana* (Prymnesiophyceae) and *Thalassiosira pseudonana* (Bacillariophyceae). Journal of Phycology 45 (4), 864–872.

Kattner, G., Brockmann, U.H., 1980. Semi-automated method for the determination of particulate phosphorus in the marine environment. Fresenius Zeitschrift für Analytische Chemie 301, 14–16.

Kruskopf, M.M., Du Plessis, S., 2004. Induction of both acid and alkaline phosphatase activity in two green-algae (Chlorophyceae) in low N and P concentrations. Hydrobiologia 513 (1), 59–70.

La Claire, J., 2006. Analysis of expressed sequence tags from the harmful alga, *Prymnesium parvum* (Prymnesiophyceae, Haptophyta). Marine Biotechnology 8 (5), 534–546.

Larsen, A., Bryant, S., 1998. Growth rate and toxicity of *Prymnesium parvum* and *Prymnesium patelliferum* (Haptophyta) in response to changes in salinity, light and temperature. Sarsia 83, 409–418.

Larsen, A., Eikrem, W., Paasche, E., 1993. Growth and toxicity in *Prymnesium patelliferum* (Prymnesiophyceae) isolated from Norwegian waters. Canadian Journal of Botany 71, 1357–1362.

Legrand, C., Johansson, N., Johnsen, G., Borsheim, K.Y., Graneli, E., 2001. Phagotrophy and toxicity variation in the mixotrophic *Prymnesium patelliferum* (Haptophyceae). Limnology and Oceanography 46 (5), 1208–1214.

Lindehoff, E., Granéli, E., Granéli, W., 2009. Effect of tertiary sewage effluent additions on *Prymnesium parvum* cell toxicity and stable isotope ratios. Harmful Algae 8 (2), 247–253.

Lindholm, T., Öhman, P., Kurki-Helasmo, K., Kincaid, B., Meriluoto, J., 1999. Toxic algae and fish mortality in a brackish-water lake in Åland, SW Finland. Hydrobiologia 397 (0), 109–120.

Lindholm, T., Virtanen, T., 1992. A bloom of *Prymnesium parvum* Carter in a small coastal inlet in Dragsfjärd, southwestern Finland. Environmental Toxicology and Water Quality 7 (2), 165–170.

Lunn, D., Spiegelhalter, D., Thomas, A., Best, N., 2009. The BUGS project: evolution, critique and future directions. Statistics in Medicine 28 (25), 3049–3067.

McDonald, S.M., Plant, J.N., Worden, A.Z., 2010. The mixed lineage nature of nitrogen transport and assimilation in marine eukaryotic phytoplankton: a case study of *Micromonas*. Molecular Biology and Evolution 27 (10), 2268–2283.

Meldahl, A.S., Kvernstuen, J., Grasbakken, G.J., Edvardsen, B., Fonnum, F., 1995. Toxic activity of *Prymnesium* spp. and *Chrysochromulina* spp. tested by different test methods. Harmful Marine Algal Blooms 315–320.

Michaloudi, E., Moustaka-Gouni, M., Gkelis, S., Pantelidakis, K., 2009. Plankton community structure during an ecosystem disruptive algal bloom of *Prymnesium parvum*. Journal of Plankton Research 31 (3), 301–309.

Moestrup, O., 1994. Economic aspects: 'blooms', nuisance species, and toxins. In: Green, J.C., Leadbeater, B.S.C. (Eds.), The Haptophyte Algae. Clarendon Press, Oxford, pp. 265–285.

Moseley, J.L., Chang, C.-W., Grossman, A.R., 2006. Genome-based approaches to understanding phosphorus deprivation responses and PSR1 control in *Chlamydomonas reinhardtii*. Eukaryotic Cell 5 (1), 26–44.

Muller, J., Szklarczyk, D., Julien, P., Letunic, I., Roth, A., Kuhn, M., Powell, S., von Mering, C., Doerks, T., Jensen, L.J., Bork, P., 2010. eggNOG v2.0: extending the evolutionary genealogy of genes with enhanced non-supervised orthologous groups, species and functional annotations. Nucleic Acids Research 38 (Suppl. 1), D190–D195.

Nygaard, K., Tobiesen, A., 1993. Bacterivory in algae: a survival strategy during nutrient limitation. Limnology and Oceanography 38 (2), 273–279.

Palenik, B., Morel, F.M.M., 1991. Amine oxidases of marine phytoplankton. Applied and Environmental Microbiology 57 (8), 2440–2443.

Parker, M.S., Armbrust, E.V., 2005. Synergistic effects of light, temperature, and nitrogen source on transcription of genes for carbon and nitrogen metabolism in the centric diatom *Thalassiosira pseudonana* (Bacillariophyceae). Journal of Phycology 41 (6), 1142–1153.

Patron, N.J., Waller, R.F., Keeling, P.J., 2006. A tertiary plastid uses genes from two endosymbionts. Journal of Molecular Biology 357 (5), 1373–1382.

Pinney, J.W., Shirley, M.W., McConkey, G.A., Westhead, D.R., 2005. metaSHARK: software for automated metabolic network prediction from DNA sequence and its application to the genomes of *Plasmodium falciparum* and *Eimeria tenella*. Nucleic Acids Research 33 (4), 1399–1409.

Riegman, R., Stolte, W., Noordeloos, A.A.M., Slezak, D., 2000. Nutrient uptake and alkaline phosphatase (ec 3:1:3:1) activity of *Emiliania huxleyi* (Prymnesiophyceae) during growth under N and P limitation in continuous cultures. Journal of Phycology 36 (1), 87–96.

Roelke, D.L., Schwierzke, L., Brooks, B.W., Grover, J.P., Errera, R.M., Valenti, T.W., Pinckney, J.L., 2010. Factors influencing *Prymnesium parvum* population dynamics during bloom initiation: results from in-lake mesocosm experiments. JAWRA Journal of the American Water Resources Association 46 (1), 76–91.

Saeed, A.I., Bhagabati, N.K., Braisted, J.C., Liang, W., Sharov, V., Howe, E.A., Li, J., Thiagarajan, M., White, J.A., Quackenbush, J., 2006. TM4 microarray software suite. In: Alan, K., Brian, O. (Eds.), Methods in Enzymology. Academic Press, pp. 134–193.

Sanders, J.G., Windom, H.L., 1980. The uptake and reduction of arsenic species by marine algae. Estuarine and Coastal Marine Science 10 (5), 555–567.

Schug, K.A., Skingel, T.R., Spencer, S.E., Serrano, C.A., Le, C.Q., Schug, C.A., Valenti Jr., T.W., Brooks, B.W., Mydlarz, L.D., Grover, J.P., 2010. Hemolysis, fish mortality, and LC-ESI-MS of cultured crude and fractionated golden alga (*Prymnesium parvum*). JAWRA Journal of the American Water Resources Association 46 (1), 33–44.

Sharkey, T.D., Laporte, M., Lu, Y., Weise, S., Weber, A.P.M., 2004. Engineering plants for elevated CO_2: a relationship between starch degradation and sugar sensing. Plant Biology 6 (3), 280–288.

Sillo, A., Bloomfield, G., Balest, A., Balbo, A., Pergolizzi, B., Peracino, B., Skelton, J., Ivens, A., Bozzaro, S., 2008. Genome-wide transcriptional changes induced by phagocytosis or growth on bacteria in *Dictyostelium*. BMC Genomics 9 (1), 291.

Skovgaard, A., Hansen, P.J., 2003. Food uptake in the harmful alga *Prymnesium parvum* mediated by excreted toxins. Limnology and Oceanography 48 (3), 1161–1166.

Sopanen, S., Koski, M., Uronen, P., Kuuppo, P., Lehtinen, S., Legrand, C., Tamminen, T., 2008. Prymnesium parvum exotoxins affect the grazing and viability of the calanoid copepod *Eurytemora affinis*. Marine Ecology Progress Series 361, 191–202.

Stoecker, D.K., 1998. Conceptual models of mixotrophy in planktonic protists and some ecological and evolutionary implications. European Journal of Protistology 34 (3), 281–290.

Storey, J.D., 2003. The positive false discovery rate: a Bayesian interpretation and the *q*-value. Annals of Statistics 31 (6), 2013–2035.

Team, R.D.C., 2008. R: A Language and Environment for Statistical Computing. R Foundation for Statistical Computing.
Ticconi, C.A., Abel, S., 2004. Short on phosphate: plant surveillance and countermeasures. Trends in Plant Science 9 (11), 548–555.
Tillmann, U., 1998. Phagotrophy by a plastidic haptophyte, *Prymnesium patelliferum*. Aquatic Microbial Ecology 14 (2), 155–160.
Tillmann, U., 2003. Kill and eat your predator: a winning strategy of the planktonic flagellate *Prymnesium parvum*. Aquatic Microbial Ecology 32, 73–84.
Tillmann, U., Alpermann, T., John, U., Cembella, A., 2008. Allelochemical interactions and short-term effects of the dinoflagellate *Alexandrium* on selected photoautotrophic and heterotrophic protists. Harmful Algae 7 (1), 52–64.
Uronen, P., Kuuppo, P., Legrand, C., Tamminen, T., 2007. Allelopathic effects of toxic Haptophyte *Prymnesium parvum* lead to release of dissolved organic carbon and increase in bacterial biomass. Microbial Ecology 54 (1), 183–193.
Uronen, P., Lehtinen, S., Legrand, C., Kuuppo, P., Tamminen, T., 2005. Haemolytic activity and allelopathy of the haptophyte *Prymnesium parvum* in nutrient-limited and balanced growth conditions. Marine Ecology Progress Series 299, 137–148.
Valenti Jr., T.W., James, S.V., Lahousse, M.J., Schug, K.A., Roelke, D.L., Grover, J.P., Brooks, B.W., 2010. A mechanistic explanation for pH-dependent ambient aquatic toxicity of *Prymnesium parvum* Carter. Toxicon 55 (5), 990–998.
von Dassow, P., Ogata, H., Probert, I., Wincker, P., Da Silva, C., Audic, S., Claverie, J.-M., de Vargas, C., 2009. Transcriptome analysis of functional differentiation between haploid and diploid cells of *Emiliania huxleyi*, a globally significant photosynthetic calcifying cell. Genome Biology 10 (10), R114.
Wurch, L.L., Haley, S.T., Orchard, E.D., Gobler, C.J., Dyhrman, S.T., 2011. Nutrient-regulated transcriptional responses in the brown tide-forming alga *Aureococcus anophagefferens*. Environmental Microbiology 13 (2), 468–481.
Wykoff, D.D., Grossman, A.R., Weeks, D.P., Usuda, H., Shimogawara, K., 1999. Psr1, a nuclear localized protein that regulates phosphorus metabolism in *Chlamydomonas*. Proceedings of the National Academy of Sciences 96 (26), 15336–15341.
Xu, Y., Selaru, F.M., Yin, J., Zou, T.T., Shustova, V., Mori, Y., Sato, F., Liu, T.C., Olaru, A., Wang, S., Kimos, M.C., Perry, K., Desai, K., Greenwald, B.D., Krasna, M.J., Shibata, D., Abraham, J.M., Meltzer, S.J., 2002. Artificial neural networks and gene filtering distinguish between global gene expression profiles of Barrett's esophagus and esophageal cancer. Cancer Research 62 (12), 3493–3497.
Yang, H.-C., Cheng, J., Finan, T.M., Rosen, B.P., Bhattacharjee, H., 2005. Novel pathway for arsenic detoxification in the legume symbiont *Sinorhizobium meliloti*. Journal of Bacteriology 187 (20), 6991–6997.
Yang, I., Beszteri, S., Tillmann, U., Cembella, A., John, U., 2011. Growth- and nutrient-dependent gene expression in *Alexandrium minutum*. Harmful Algae 12, 55–69.
Yasumoto, T., Underdahl, B., Aune, T., Hormazabal, V., Skulberg, O.M., 1990. Screening for hemolytic activity and ichtyotoxic components of *Chrysochromulina polylepis* and *Gyrodinium aureolum* from Norwegian coastal waters. In: Granéli, E., Sundström, B., Edler, L., Anderson, D.M. (Eds.), Toxic Marine Phytoplankton. Elsevier, New York, pp. 436–440.